PAPER • OPEN ACCESS

Burst pressure design of the cargo tank used in a novel large subsea freight-glider

To cite this article: Y. Xing 2021 *IOP Conf. Ser.: Mater. Sci. Eng.* **1201** 012014

Burst pressure design of the cargo tank used in a novel large subsea freight-glider

Y. Xing

University of Stavanger, Norway

Corresponding author: yihan.xing@uis.no

Abstract. This paper presents the burst pressure design of the cargo tank used in the University of Stavanger (UiS) Subsea Freight-Glider (USFG). The USFG is an innovative large underwater cargo glider drone that is 50 m long and has a DWT of 1500 ton. It uses variable-buoyancy propulsion instead of traditional propellers for movement. This is an extremely efficient propulsion method and allows the USFG to achieve an average energy consumption of less than 10 kW. Structural weight is a premium as the USFG is required to be neutrally buoyant in water. Therefore, the design of the cargo tank which is the largest component in the USFG needs to be optimal for minimal structural weight. One approach used in design optimisation is to utilise design codes and/or methods that are more precise and therefore allow for lower safety margins. This approach will be investigated in this paper for the burst pressure design of the cargo tank. The different parts of ASME BPVC codes will be compared. The sensitivity of the codes to changes in design parameters is also investigated. Lastly, some comments on the use of reliability methods to further optimise the design are also presented.

Nomenclature

ASME	Americal Society of Mechanical Engineers
BPVC	Boiler and pressure vessel code
D, D_o	Outer diameter
D_i	Inner diameter
DBA	Design by analysis
DBR	Design by rules
E	Weld efficiency factor
EP	Elastic-plastic
F	Additional equivalent stress
LE	Linear-elastic
LL	Limit-load
m_2	ASME material constant
P, P_D	Design pressure
P_b	Primary bending equivalent stress
P_L	Local primary membrane stress
P_m	Primary membrane equivalent stress
Q	Secondary equivalent stress
R	Ratio of yield strength vs tensile strength
S	Allowable stress

S_t, S_u	Tensile stress
S_y	Yield stress
SST	Subsea shuttle tanker
t	Thickness
t_{min}	Minimum wall thickness
$t_{min,final}$	Minimum wall thickness required by code
USFG	UiS Subsea Freight-Glider
Y	Diameter ratio
α	Shape factor
α_{sl}	ASME material constant
ε_{cf}	Forming strain
ε_{peq}	Equivalent plastic strain
ε_L	Triaxial limiting strain
ε_{LU}	Uniaxial strain limit
σ_1, σ_2, σ_3	Principal stresses
σ_e	Equivalent stress

1. Introduction

Xing [1] proposed a novel subsea-freight glider system as a cost-effective alternative to tanker ships and pipelines in the transportation of CO2. This subsea-freight glider is illustrated in Figure 1 and is called the UiS Subsea Freight-Glider (USFG). It is a 50 m long vessel with a DWT displacement of 1500 tons and can carry 785 ton of CO2. The USFG uses variable-buoyancy propulsion instead of the traditional propellers. It changes its ballast to provide negative or positive net buoyancy to allow it to float or sink in water. The hydrodynamic wings generate horizontal thrust through the vertical motion and propelling the USFG forward. The working principle of USFG is illustrated in Figure 2. This is an extremely efficient propulsion method which gives an average energy consumption and a net transport economy (NTE) of less than 10 kW and 0.5, respectively.

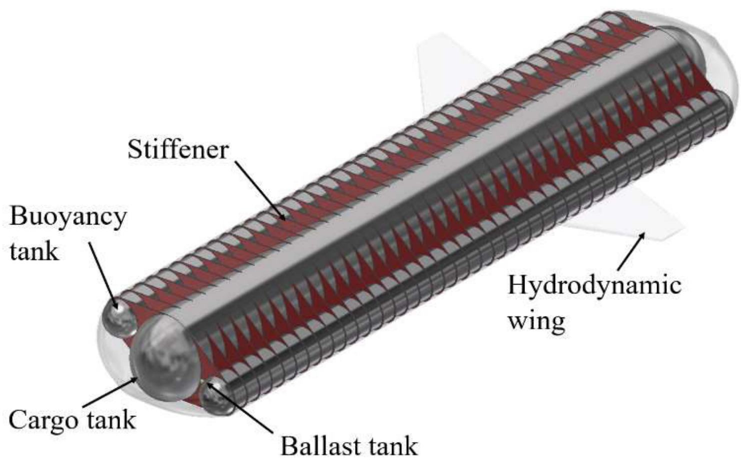

Figure 1. UiS subsea freight-glider

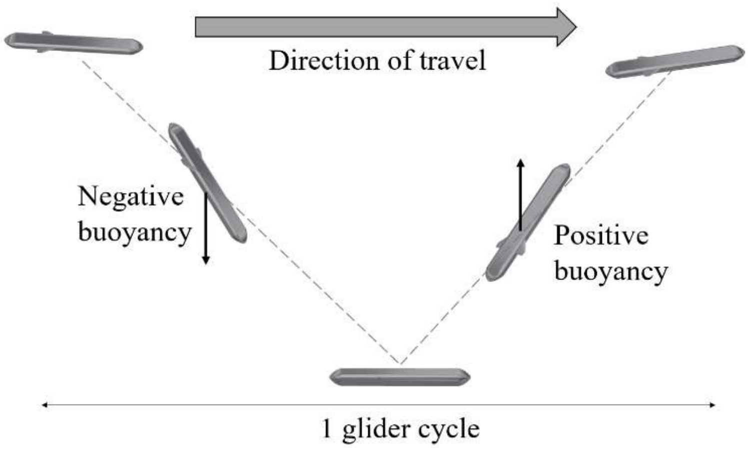

Figure 2. Working principle of UiS subsea freight-glider

The design of a large underwater vehicle such as the USFG is very challenging since the vehicle must be neutrally buoyant, i.e., weight is must be equal to buoyancy for the vehicle not to sink or float in water. Like other submarines, the USFG cannot simply accommodate changes in weight by adjusting its draught, i.e., without any changes to the ship hull geometry [2]. The equivalent density of the USFG must be equal to that of seawater. Any changes in weight must be compensated by changes in the volume (and therefore geometry) which will in turn increase the weight. Structural weight is a premium that is extremely attractive to minimize.

The USFG is essentially a large pressure vessel and the optimization of its pressure vessel design will naturally lead to a large weight reduction. One approach is to utilize design codes and/or methods that are more precise and therefore allow for lower safety margins. This approach will be investigated in this paper for the burst pressure design of the cargo tank in the USFG. Different parts of ASME BPVC codes will be compared. The sensitivity of the codes to changes in design parameters is also investigated. Lastly, some comments on the use of reliability methods to further optimize the design are also presented. The findings from this paper provide insights into burst pressure design for other large underwater cargo vehicles where weight is a premium. These include the recently proposed Equinor and UiS subsea shuttles [3][4][5].

2. Design description

The main design parameters of the USFG are presented in Table 1. These parameters were derived using a design optimization process combined with a probabilistic analysis in Xing [1].

Table 1. Main design parameter [1]

Parameter	Value	Unit
Vessel length	50	m
Cargo tank diameter	5.0	m
Buoyancy tank diameter	2.2	m
Dead weight ton	1533	ton
Strucutral weight	470	ton
Cargo weight	785	ton
Ballast fraction	0.15	%
Diving depth	200	m
Glide path angle	38	°
Wing area	20	m^2
Volumetric drag coefficient	0.1	-
Ballast pump capacity	2000	m^3/h
Pumping time / cycle	< 5 % of half cycle	-
Horizontal speed	1	m/s
Average power	< 10	kW
Net transport economy	< 0.5	-

The USFG has the following main components as presented in Figure 1:

(i) A large cylindrical steel cargo tank carrying liquid CO2 in middle;
(ii) Two smaller cylindrical steel buoyancy tanks on the sides that are filled with air to allow for a neutrally buoyant vessel;
(iii) The cargo and buoyancy tanks utilize a common steel stiffening structure for increased collapse pressure capacity;
(iv) Four small steel ballast tanks, two at the front and two at the back for net buoyancy and pitch/roll angle control;
(v) A streamlined outer hull made of composite material for low hydrodynamic drag. The space between the outer hull and internal pressure hulls are water-filled, therefore the outer hull does not require a high-pressure collapse capacity design; and
(vi) Two small hydrodynamic wings made of composite material provide lift. The wings have ailerons for pitch/roll control of the vessel.

2.1. CO_2 properties

The SST transports CO2 in the saturated liquid state at pressures and temperatures of 35 - 55 bar and 0 - 20 °C, respectively. The advantage of the saturated liquid state is that the temperature and pressure are passively regulated with the environment. This means no external energy is required. This approach is also used in the UiS subsea shuttle [6].

2.2. Internal tank structures and cargo tank

The USFG uses a ring-stiffened internal tank structure. The internal tank arrangement is presented in Figure 3. The cargo tank must handle both internal and external pressure. The buoyancy tanks' main purpose is to provide buoyancy and is filled with air at atmospheric pressure; they handle only external hydrostatic pressure.

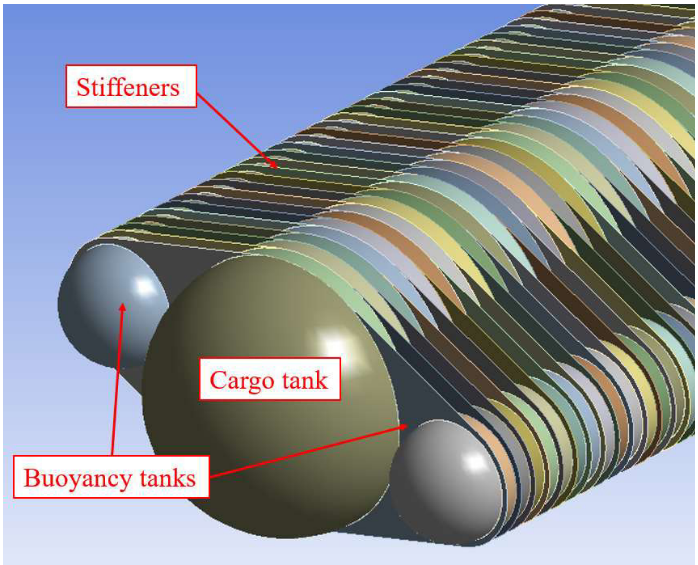

Figure 3. Internal tank arrangement

The cargo tank is the component of interest in this paper. Based on the CO2 properties discussed in Section 2.1. , the cargo tank's design parameters are therefore:

- Design pressure = 55 bar
- Design temperature = 0 to 20 °C

The baseline geometry of the internal tank structures was derived using a design optimisation process with its robustness quantified via a probabilistic analysis in Xing [1]. The parameters obtained are illustrated in Figure 4 and presented in Table 2. The descriptions of the parameters are:

- d: diameter of the buoyancy tank
- x: distance between the stiffeners
- x2: shortest distance between the cargo tank and the buoyancy tanks
- h: height of stiffener around the buoyancy tank
- t1, t2, t3, thicknesses of the cargo tank, buoyancy tank and stiffener, respectively

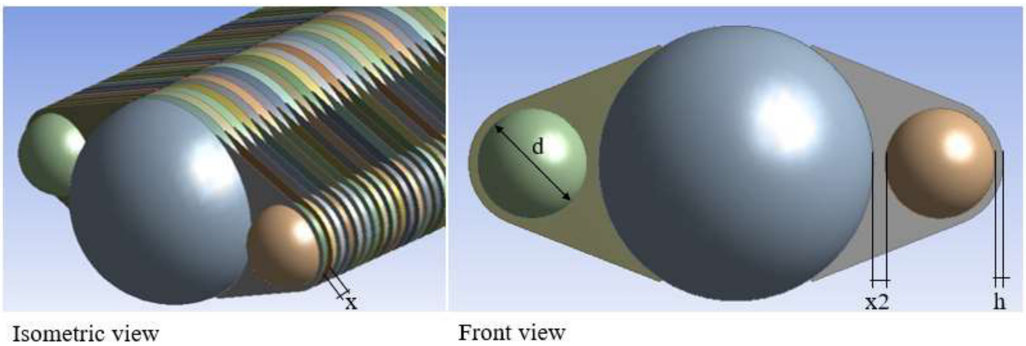

Figure 4. Baseline parameters of the internal tank structures

Table 2. Baseline parameters of the internal tank structures

d [mm]	x [mm]	x2 [mm]	h [mm]	t1 [mm]	t2 [mm]	t3 [mm]	W [ton]
2194	372	144	119	50.0	12.2	10.7	441

2.3. Material

SA-738 Grade B is chosen as the material for the internal tank structures. It is a high strength carbon steel widely used in welded pressure vessels subjected to moderate or lower temperatures. The properties of SA-738 Grade B are listed in Table 3.

Table 3. Properties of SA-738 Grade B, Ref. ASME II-D [11]

Parameter	Value	Unit
Yield strength	414	MPa
Tensile strength	586	MPa
Allowable stress, ASME VIII-1	166	MPa
Allowable stress, ASME VIII-2	244	MPa
Young's modulus	206	Gpa
Possion ratio	0.3	-
$m_2 = 0.6 \cdot (1 - R)$	0.177	-
α_{sl}	2.2	-

The elastic-plastic methods described in Sections 3.2.3. and 3.2.5. for ASME VIII-2 and VIII-3, respectively require the use of nonlinear elastic-plastic stress-strain curves developed in accordance with ASME VIII-2 Annex 3-D. The stress-strain curve for SA-738 Grade B used in this paper is plotted in Figure 5.

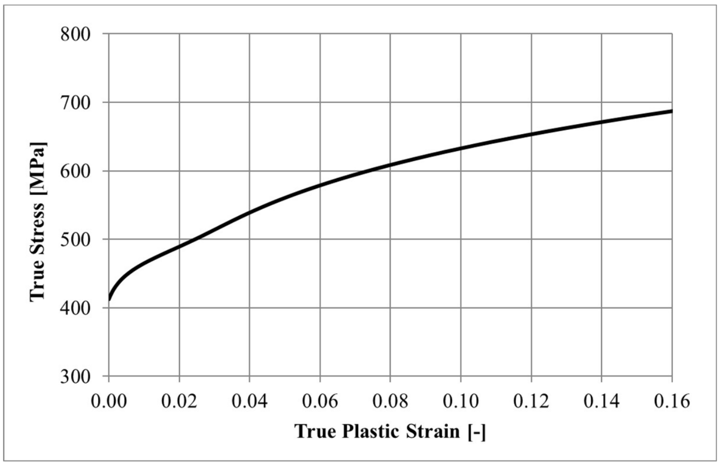

Figure 5. Stress-Strain Curve for SA-738 Grade B

3. Burst design methodology

The burst design of the cargo tank can be performed using different methods in ASME BPVCs. These are illustrated in Figure 6.

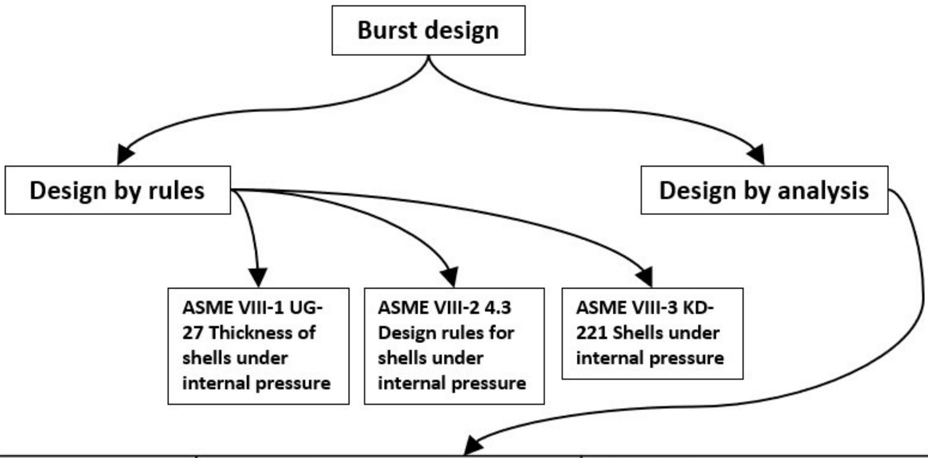

	ASME VIII-2		ASME VIII-3	
	Protection against global collapse	**Protection against local failure**	**Protection against global collapse**	**Protection against local failure**
Linear elastic analysis	5.2.2 Elastic stress analysis method	5.3.2 Elastic analysis – Triaxial stress limit	KD-240 Linear elastic analysis	
Limit-load analysis	5.2.3 Limit-load analysis method	5.3.2 Elastic analysis – Triaxial stress limit **OR** 5.3.3 Elastic-plastic analysis – Local strain limit		
Elastic-plastic analysis	5.2.4 Elastic-plastic stress analysis method	5.3.3 Elastic-plastic analysis – Local strain limit	KD-231 Elastic-plastic analysis method	KD-232 Protection against local failure

Figure 6. Different ASME VIII burst design methodologies

There are three ASME VIII parts, ASME VIII-1 [7], ASME VIII-2 [8] and ASME VIII-3 [9]. They provide design calculation methods in order of increasing accuracy and therefore decreasing safety factor levels. ASME VIII-1 and VIII-2 rules are very popular and are used in more than 80 % of pressure vessels constructed in a survey conducted by ASME Standards Technology [10]. It is also a requirement that the materials used be listed in ASME II [11] when the ASME BPVCs are utilised.

In general, there are three types of design methods provided by ASME VIII, namely design by rules (DBR), design by testing and design by analysis (DBA). DBR methods typically employ semi-empirical-analytical formula in the design calculations. They also restrict the type of geometries to standard geometries. All three parts of ASME VIII have DBR methods. The corresponding DBR sections of the codes are presented in Figure 6. Design by testing as the name suggests is to use physical testing to determine the design pressure of pressure vessels that have non-standard geometries. This is no longer a common method in today's pressure vessel design after the predominant use of finite element software in mechanical engineering. The design by testing method will not be considered in this paper. DBA is to use computational analysis for the design exercise. The analysis methods used can be the linear elastic, limit-load, and elastic-plastic analysis methods. The differences between these three methods are in the definition of the materials and non-linear geometry. In a linear elastic analysis, linear material models and a linear finite element (FE) formulation are used. In a limit-load analysis, elastic-perfectly-plastic material models and a FE formulation that handles non-linear geometry are used. Lastly, an elastic-plastic analysis uses elastic-plastic materials that account for the full strain-hardening properties in monotonic loading and uses a FE formulation that handles non-linear geometry. For burst design, protection against three failure modes which are global collapse, local failure and cyclic loading are to be considered. Protection against cyclic loading is not considered in this paper. The corresponding parts of ASME VIII-2 and VIII-3 for DBA are presented in Figure 6. ASME VIII-1 does not have a DBA section.

One interesting note briefly mentioned here is that DBA methods may not lead to increased pressure capacities calculated for the design. This is the case for the USFG cargo tank and is further discussed in Section 5.1.

3.1. Design by rules methods

DBR methods from ASME VIII-1 [7], ASME VIII-2 [8] and ASME VIII-3 [9] are used. These are presented in Section 3.1.1. , 3.1.2. and 3.1.3. respectively.

3.1.1. ASME VIII-1 UG-27 Thickness of shells under internal pressure. This section calculates the required minimum thickness of shells under internal pressure. The calculations that are relevant for the USFG cargo tank are (c)(1) Cylindrical shells, Circumferential stress, (c)(2) Cylindrical shells, Longitudinal stress and (d) Spherical shells. The minimum thicknesses corresponding to these parts are presented below in equations (1) to (3), respectively. A weld efficiency, E of 1.0 is used in the calculations.

(c)(1) Cylindrical shells, Circumferential stress

$$t = \frac{PD}{2(SE - 0.6P)} \quad (1)$$

(c)(2) Cylindrical shells, Longitudinal stress

$$t = \frac{PD}{2(2SE + 0.4P)} \quad (2)$$

(d) Spherical shells

$$t = \frac{PD}{2(2SE - 0.2P)} \quad (3)$$

The maximum value of minimum thicknesses calculated from equations (1) to (3) will provide the shell thickness for the cargo tank that will meet ASME VIII-1 UG-27.

3.1.2. ASME VIII-2 4.3 Design rules for shells under internal pressure. Similarly, this section also calculates the required minimum thickness of shells under internal pressure. The calculations that are relevant for the USFG cargo tank are 4.3.3.1 Cylinder shells, required thickness and 4.3.5.1 Spherical shells and hemispherical heads, Required thickness. The minimum thicknesses corresponding to these parts are presented below in equations (4) and (5), respectively.

4.3.3.1 Cylindrical shells, Required thickness

$$t = \frac{D}{2}\left(e^{\frac{P}{SE}} - 1\right) \quad (4)$$

4.3.5.1 Spherical shells and hemispherical heads, Required thickness

$$t = \frac{D}{2}\left(e^{\frac{0.5P}{SE}} - 1\right) \quad (5)$$

3.1.3. ASME VIII-3 KD-220 Equations for cylindrical and spherical shells. ASME VIII-3 uses the definition of diameter ratio, Y instead of minimum thickness in the design calculations. Y is defined as the ratio between D_O and D_I, which are the outer and inner diameters, respectively. ASME VIII-3 differentiates between $Y \leq 2.85$ and $Y > 2.85$. For a thin wall pressure vessel such as the USFG cargo tank, Y will be close to 1.0, i.e., $Y \leq 2.85$. The relevant calculations are KD-221.1 Cylindrical monobloc shells and KD-221.3 Spherical monobloc shells. The design pressures for a diameter ratio, Y for $Y \leq 2.85$ corresponding to these parts are presented in equations (6) and (7), respectively.

KD-221.1 Cylindrical monobloc shells

$$P_D = min\left(\left[2.5856\left(S_y\right)\left(Y^{0.268}-1\right)\right],\left[1.0773\left(S_y+S_u\right)\left(Y^{0.268}-1\right)\right]\right) \tag{6}$$

KD-221.3 Spherical monobloc shells

$$P_D = min\left(\left[\frac{\sqrt{3}}{1.25}\left(S_y\right) ln(Y)\right],\left[\frac{1}{\sqrt{3}}\left(S_y+S_u\right) ln(Y)\right]\right) \tag{7}$$

Re-writing equations (6) and (7) to make minimum thickness the subject leads to equations (8) and (9), respectively. This means to substitute $Y = D_O/D_I = D_O/(D_O\text{-}2t)$ and make t the subject.

Minimum thickness for KD-221.1 Cylindrical monobloc shells

$$t = max\left(\left[\frac{D_o}{2}\left(1-\left(\frac{P_D}{2.5856S_y}+1\right)^{-\left(\frac{1}{0.268}\right)}\right)\right],\left[\frac{D_o}{2}\left(1-\left(\frac{P_D}{1.0773\left(S_y+S_u\right)}+1\right)^{-\left(\frac{1}{0.268}\right)}\right)\right]\right) \tag{8}$$

Minimum thickness for KD-221.3 Spherical monobloc shells

$$t = max\left(\left[\frac{D_o}{2}\left(1-e^{-\left(\frac{1.25P_D}{\sqrt{3}S_y}\right)}\right)\right],\left[\frac{D_o}{2}\left(1-e^{-\left(\frac{\sqrt{3}P_D}{S_y+S_u}\right)}\right)\right]\right) \tag{9}$$

3.2. Design by analysis methods

DBA methods from ASME VIII-2 [8] and ASME VIII-3 [9] are used. For burst design, the relevant design calculations must be performed for the protection against plastic collapse, protection against local failure. Correspondingly, the relevant sections in ASME VIII-2 are 5.2 – Protection against global collapse and 5.3 – Protection against local failure and the relevant sections in ASME VIII-3 are KD-230 – Elastic-plastic analysis and KD-240 – Linear elastic analysis.

3.2.1. ASME VIII-2 Linear elastic method. Linear FE analyses are performed using linear elastic material. No additional load factors are applied. For the protection against global collapse check, the stresses calculated are categorised into the following groups:

- General primary membrane equivalent stress, P_m
- Local primary membrane stress, P_L
- Primary bending equivalent stress, P_b

- Secondary equivalent stress, Q
- Additional equivalent stress produced by a stress concentration or a thermal stress over and above the nominal $(P + Q)$, F

The following criteria are to be met:

- $P_m \leq S$
- $P_L \leq S_{PL}$
- $(P_L + P_b) \leq S_{PL}$

S_{PL} is computed as the larger of $1.5 \cdot S$ and S_y. However, $S_{PL} = 1.5 \cdot S$ if $S_y/S_t > 0.7$. For the protection against local failure check, the design is ok if the triaxial stress limit is fulfilled:

- $(\sigma_1 + \sigma_2 + \sigma_3) \leq 4 \cdot S$

3.2.2. ASME VIII-2 Limit-load method. For the protection against global collapse check, FE analyses with non-linear geometry are performed using elastic-perfectly-plastic material. The design check is fulfilled if the FE solution converges when a load factor of 1.5 is applied. For the protection against local failure check, linear elastic method (Ref. Section 3.2.1. , triaxial stress limit) or the elastic-plastic method (Ref. Section 3.2.3. , local strain limit) can be used.

3.2.3. ASME VIII-2 Elastic-plastic method. FE analyses with non-linear geometry are performed using elastic-plastic material. The design check for the protection against global collapse check is fulfilled if the FE solution converges when a load factor of 2.4 is applied. For the protection against local failure check, the local strain limit must be fulfilled for a load factor of 1.7:

- $\varepsilon_{peq} + \varepsilon_{cf} \leq \varepsilon_L$

$$\varepsilon_L = \varepsilon_{Lu} \cdot exp\left[-\left(\frac{\alpha_{sl}}{1+m_2}\right)\left(\frac{\sigma_1+\sigma_2+\sigma_3}{3\sigma_e}-\frac{1}{3}\right)\right] \quad (10)$$

In this paper, $\varepsilon_{Lu} = m_2$.

3.2.4. ASME VIII-3 KD-240 Linear elastic method. Like ASME VIII-2, linear FE analyses are performed using linear elastic material. No additional load factors are applied. For the protection against global collapse check, the stresses calculated are categorised into the same groups, P_m, P_L, P_b, Q and F. The criteria to be met are however different from ASME VIII-2 and are listed below:

- $P_m \leq S_y/1.5$
- $P_L \leq S_y$
- $(P_L + P_b) \leq \alpha \cdot S_y/1.5$

α is the shape factor and is the ratio of the moment that produces a full plastic section to the bending moment that produces initial yielding at the extreme fibres of the section. For the protection against local failure check, the design is ok if the following triaxial stress limit is fulfilled:

- $(\sigma_1 + \sigma_2 + \sigma_3) \leq 2.5 \cdot S_y$

Recall that the limit is $4 \cdot S$ in ASME VIII-2 (Ref. Section 3.2.1.).

3.2.5. ASME VIII-3 KD-230 Elastic-plastic method. Like ASME VIII-2, FE analyses with non-linear geometry are performed using elastic-plastic material. The procedures are like ASME VIII-2 except that the load factors applied are different. For protection against global collapse, a load factor of 1.8 is used, while for protection against local failure, a load factor of 1.28 is used.

4. Finite element model

The finite element model utilised for the DBA checks is presented in this section. Ansys 2020 R2 [12] is used. A 3D thin shell model of the entire internal tank structure is implemented. The loads and boundary conditions applied are presented in Figure 7. As observed, the pressure is applied on the inside of the cargo tank surfaces. A fixed support is applied at a small edge at one end of the structure.

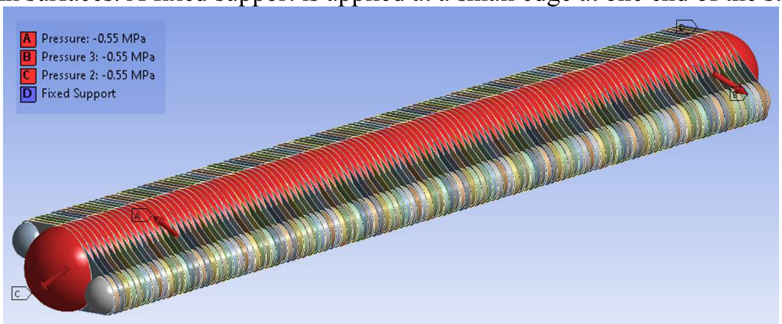

Figure 7. Finite element model - Loads and boundary conditions

SHELL181 elements, which are 4-node elements with six degrees of freedom at each node are used. The mesh details are presented in Figure 8. There are 419678 elements with 382930 nodes.

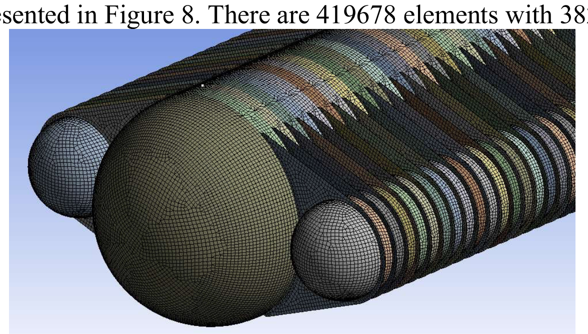

Figure 8. Finite element model mesh details

An example stress plot is presented in Figure 9. This stress plot presents the membrane stress that is used in ASME VIII-2 and VIII-3 DBR LE checks.

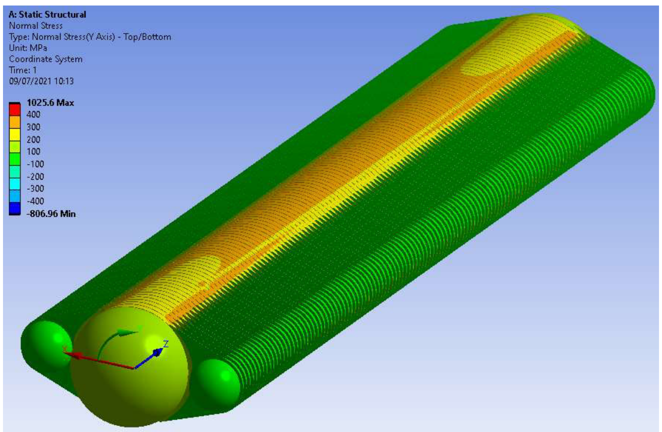

Figure 9. Example stress plot – Membrane stress from linear elastic analysis, P = 55 bar

5. Results and discussions

5.1. Code comparison

The minimum required wall thicknesses calculated using different ASME BPVC sections are presented in Table 4. The smallest wall thickness is 47.4 mm and is calculated by ASME VIII-3 DBR method. The largest wall thickness is 83.7 mm and is calculated by ASME VIII-1 DBR method. It is noted that it was not possible to determine the pressure load where the triaxial strain limit is met for the limit-load and elastic-plastic methods. This is because the structure collapses globally at a significantly lower pressure load, i.e., the FE solution breaks down way before the triaxial strain limit is met.

Table 4. Results from code comparison

Design code	Design method	Section	t_{min} [mm]	$t_{min, final}$ [mm]	Weight [ton]
ASME VIII-1	DBR	UG-27 (c)(1) – Cylinderical shells – Circumferential stress	83.7	83.7	628
		UG-27 (c)(2) - Cylinderical shells – Longitudinal stress	40.8		
		UG-27 (d) Spherical shells	41.2		
ASME VIII-2		4.3.3.1 Cylindrical shells, Required thickness	57.0	57.0	480
		4.3.5.1 Spherical shells and hemispherical heads, Required thickness	28.3		
ASME VIII-3		KD-221.1 Cylindrical monobloc shells	47.4	47.4	426
		KD-221.3 Spherical monobloc shells	23.9		
ASME VIII-2	DBA – Linear elastic	5.2 – Protection against global collapse	65.7	65.7	528
		5.3 – Protection against local failure	28.4		
	DBA – Limit-load	5.2 – Protection against global collapse	48.8	48.8	434
		5.3 – Protection against local failure	-[1]		
	DBA – Elastic-plastic	5.2 – Protection against global collapse	57.4	57.4	482
		5.3 – Protection against local failure	-[1]		
ASME VIII-3	DBA – Linear elastic	KD-240 Linear elastic method – Protection against global collapse	56.7	56.7	478
		KD-240 Linear elastic method – Protection against local failure	27.4		
	DBA – Elastic-plastic	KD-230 Elastic-plastic method – Protection against global collapse	49.2	49.2	437
		KD-230 Elastic-plastic method – Protection against local failure	-[1]		

[1] FE solution breaks down way before the triaxial strain limit is met.

Important observations of the results presented in Table 4 are discussed in the following.

DBR methods: Within the same ASME part, DBR methods in general lead to the smaller wall thickness. The smallest wall thickness value of 47.4 mm is calculated by the ASME VIII-3 DBR linear elastic method giving a structural weight of 426 ton. The exception is ASME VIII-2 limit-load method.

ASME VIII-1 vs VIII-2 vs VIII-3: In general, the required wall thickness is the largest and smallest when ASME VIII-1 and ASME VIII-3 are used, respectively. This is due to the lower safety factors used in ASME VIII-2 and ASME VIII-3. For example, in DBR methods, adopting ASME VIII-2 and ASME VIII-3 leads a required wall thickness of 68 % and 56 % compared to ASME VIII-1, respectively. This leads to a weight saving of 148 ton and 202 ton when ASME VIII-2 and ASME VIII-3 are used, respectively. The weight savings are massive; it is extremely attractive to use ASME VIII-3. The weight savings are in general lesser in DBA methods. For example, using ASME VIII-3 elastic-plastic analysis leads to a wall thickness of 49.2 mm compared to 57.4 mm in ASME VIII-2 elastic-plastic analysis.

DBR vs DBA methods: On the other hand, the DBA methods do not in general lead to smaller wall thickness values except for ASME VIII-2 limit-load method. The wall thicknesses values calculated are however quite like those calculated using DBR methods. For example, in ASME VIII-2, the wall thickness calculated by DBR is 57.0 mm compared to 57.4 mm when DBA elastic-plastic method is used. This is because for thin wall pressure vessels such as in the USFG cargo tank, the stresses are relatively uniform through the material cross section. Through thickness yielding occur more easily where there is the presence of local stress concentrations. This is unlike the situation in thick wall pressure vessels where there is an abundance of material in the thick walls provide resistance to contain any plastic deformation from local stress concentrations from spreading in an uncontrolled manner. Further, the thicker walls also mean that these local stress concentrations have space to properly decay to lower stress values within the walls. Finite element analysis allows these to be modelled and considered, therefore allowing higher pressure capacities and thinner wall thicknesses. Figure 10 illustrates the comparison of stress distribution across the wall thickness between a thick and thin wall situation.

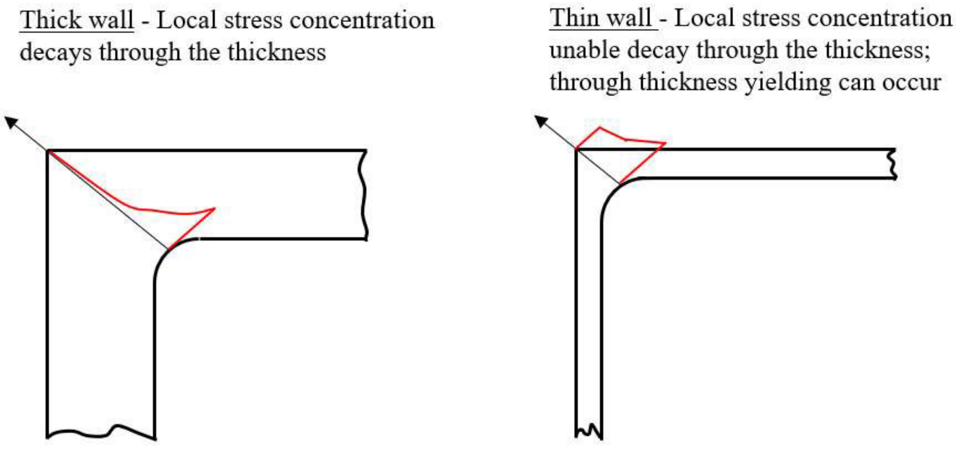

Figure 10. Stress distributions in thick and thin walls

Linear-elastic vs limit-load vs elastic-plastic: Using the more elaborate elastic-plastic methods will result in a thinner wall thickness compared to the linear elastic and limit-load methods. For example, in ASME VIII-2, the wall thickness is 65.7 mm, 48.8 mm and 57.4 mm when linear-elastic, limit-load and elastic-plastic methods are used, respectively. It is noted that the limit-load method leads to a smaller wall thickness. The reason for this is two-fold: (i) a much lower load factor of 1.5 vs 2.4 in ASME DBA for the plastic collapse check and (ii) the material used, SA-738 Grade B is a high-strength steel and has a high yield strength vs tensile strength ratio.

5.2. Sensitivity study

In this section, a study is performed to study the sensitivity of the codes due to changes in design parameters by investigating three different load conditions: (i) Base – Original design pressure, (ii) C1 – Reduced design pressure of 40 bar and (iii) C2 – Increased design pressure of 80 bar. The derived wall thicknesses and resulting internal structural tank weights are presented in Table 5 and Figure 11, respectively.

Table 5. Sensitivity study – Wall thickness vs design method employed

Design method	$t_{min,\,final}$ [mm]		
	Base	C1	C2
ASME VIII-1 DBR	83.7	60.6	122.9
ASME VIII-2 DBR	57.0	41.3	83.3
ASME VIII-3 DBR	47.4	34.6	68.5
ASME VIII-2 DBA LE	65.7	49.4	97.5
ASME VIII-2 DBA LL	48.8	35.6	69.6
ASME VIII-2 DBA EP	57.4	45.6	92.6
ASME VIII-3 DBA LE	56.7	44.3	86.7
ASME VIII-3 DBA EP	49.2	34.2	69.0

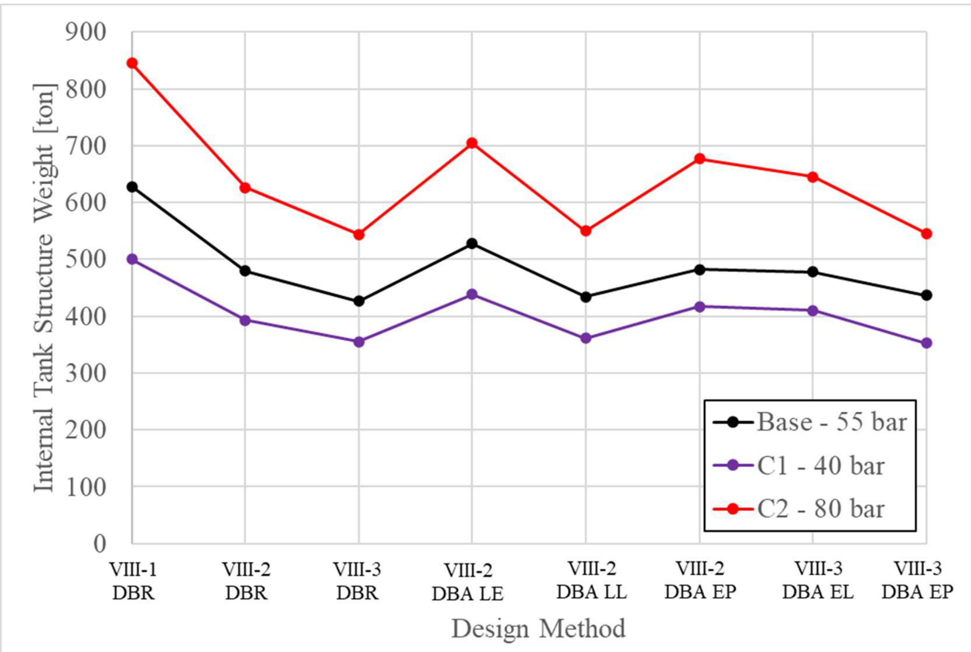

Figure 11. Sensitivity study - Weight vs design method employed

The following observations are made:

- The result trend is similar for the three cases.
- The smallest thickness and lowest weight values are calculated by the ASME VIII-3 DBR, ASME VIII-2 DBA LL and ASME VIII-3 EP methods.
- The weight savings are large when the design pressures are high. For example, a weight saving of 301 ton is obtained when the most optimal design method instead of the least optimal method is applied.

5.3. Reliability methods

The ASME BPVC codes are level I methods that adopt the allowable stress, and load and resistance factor formats. There is only one characteristic value in each uncertain parameter, e.g., characteristic, allowable or mean values. The design can adopt higher order reliability methods that utilises more information to derive a more optimal design. The level II and III methods are interesting for the USFG.

Level II methods such as the reliability index methods employ two values in each uncertain parameter, normally mean and standard deviation. The relationships between parameters are described normally using covariance.

Level III methods employ the failure of probability as a measure and therefore require information of the joint distribution of all uncertain parameters. These higher order reliability methods can be used directly to derive the design or used to calibrate the existing ASME BPVC codes. Details of these methods can be found in Madsen et al. [13], Ditlesen et al. [14] and Sundararajan [15]. There are also level IV methods; however, these require a lot of information from various non-design related aspects such as economics and consequence of failure. Due to the large amount of information required, they may not be easily employed in the initial stages of USFG development. They can however be attractive for utilisation in the second design iteration.

The burst failure of the cargo tank is dominated by global collapse. Therefore, optimisation of the design method to allow for more utilisation of the elastic-plastic portion of the material to resist global collapse will lead to the most optimal design. The ASME VIII DBA elastic-plastic methods have high load factors. These high load factors can be lowered by calibrating them with level II or III methods.

6. Conclusions

In this paper, the burst pressure design of the cargo tank in USFG is performed using different ASME BPVC methods. The most optimal design methods are found to be the ASME VIII-3 DBR, ASME VIII-2 DBA LL and ASME VIII-3 EP methods. It is concluded that significant amounts of structural weight can be saved by using the most optimal design methods. The weight savings are particularly large when the design pressure is high.

Since the burst failure of the cargo tank is dominated by global collapse, optimisation of the design method to allow for more utilisation of the material to resist global collapse will lead to the most optimal design. This will be the target for a code calibration exercise in future work.

References

[1] Xing Y 2021 A conceptual large automonous subsea freight-glider for CO2 transportation *Proc. of 40th OMAE Conf.* (Virtual: Jun 21 – 30, 2021).
[2] Burcher R, Rydill L J 1994. *Concepts in Submarine Design* (Cambridge University Press).
[3] Equinor 2019 *RD 662093 Subsea Shuttle System*.
[4] Equinor 2020 *RD 677082 Subsea Shuttle System*.
[5] Ma Y, Xing Y, Ong M C, Hemmingsen T 2021 Baseline Design of a Subsea Shuttle Tanker System for Liquid Carbon Dioxide Transportation, submitted to *Ocean Eng*.
[6] Xing Y, Ong M C, Hemmingsen T, Ellingsen K E, Reinas L 2021 Design considerations of a subsea shuttle tanker system for liquid carbon dioxide transportation. *J. Offshore Mech. Arct. Eng.* **143**(4), 045001
[7] ASME VIII-1 2019 *Boilers and Pressure Vessel Code –Rules for Construction of Pressure Vessels*
[8] ASME VIII-2 2019 *Boilers and Pressure Vessel Code – Alternative Rules for Construction of Pressure*

Vessels
[9] ASME VIII-3 2019 *Boilers and Pressure Vessel Code – Alternative Rules Construction of High Pressure Vessels*
[10] ASME Standard Technology 2006 *Comparison of Pressure Vessel Codes ASME Section VIII and EN13445* (STP-PT-007).
[11] ASME II-D 2019 *Materials - Properties*.
[12] Ansys 2020 *Theory Manual*.
[13] Madsen H O, Krenk, S, Lind, NC 2006 *Methods of Structural Safety*. (Dover: New York).
[14] Ditlevsen O, Madsen H O 1996 *Structural Reliability Methods*. (Wiley: England).
[15] Sundararajan C R 1995 *Probablistic Structural Mechanics Handbook*. (Chapman & Hall: New York).